Journal of Ceramic Processing Research. Vol. 21, No. 6, pp. 640~646 (2020)
(Received 03 April 2020, Received in revised form 19 June 2020, Accepted 16 July 2020)
https://doi.org/10.36410/jcpr.2020.21.6.640

J O U R N A L O F
Ceramic Processing Research

Fabrication and characterization of a novel foam ceramic material based on coal gasification slags

Hudie Yuan, Hongfeng Yin*, Yun Tang, Yalou Xin, Xilou Pu and Hao Zhang
Provincial Experimental Teaching Demonstration Center for Functional Materials, College of Materials Science & Engineering, Xi'an University of Architecture & Technology, 710055 Xi'an, China

In this paper, the feasibility of recycling coal gasification slag by high temperature foaming process to fabricate foal ceramic insulation board has been investigated. Silicon carbide (SiC) was added as the foam agent, and the foaming mechanism was also discussed. The results showed that utilization rate of the coal gasification prepared to the foam ceramic new wall material was up to 77% and the best dosage of SiC was 3%. Moreover, the relatively optimum parameters were obtained at the sintering temperature of 1,160 ºC for 3h with 77% slags, 20% clay and 3% SiC. Furthermore, compression strength reaches 1.18 MPa, the bulk density and heat conductivity coefficient value are 0.21 g/cm^3 and 0.05 W/(m·k), respectively.

Keywords: Foam ceramic, Walling material, Coal gasification slag; SiC, Heat conductivity coefficient.

Introduction

Recently, with the implement of related policies such as "about speeding up the enforcement advice to promote the development of green building in China", "green building build action plan" and the new "code for fire protection design of buildings", and further progress of building energy conservation [1-3]. The requirement of thermal insulation material for exterior wall of civil building is significantly increased. Especially, foam ceramic insulation board with its many advantages gradually attracted attention. Foaming ceramic is a kind of ceramic material with mine tailings and industrial solid waste as the main raw materials, adds special foaming agent, and forms amount of uniform closed pores by sintering at high temperature, which are different from the honeycomb ceramics using the open porosity technique [4-6]. As a new material, the foam ceramic possesses excellent comprehensive properties such as light-weight, high-strength, thermal insulation, fire retardant, sound insulation, and the characteristics of quick and clean construction, low building load and recyclability, etc [7-10]. Precisely, its production process can consume kinds of industrial solid waste, which is conducive to environmental protection, the foam ceramic become a new kind of green environmental protection building material in the field of new wall material and interior and exterior decoration [11-13].

The industrial solid waste can be used as the main raw material source of the foaming ceramics, which is also an important factor for the sustainable development of the foaming ceramics industry. As one kind of solid wastes, coal gasification slag is an inevitable by-product from entrained-flow coal gasification [14], which is comprised of coal ash, fluxing agent and residual carbon. The improper disposal of coal gasification slag has resulted in environmental pollution. According to the literature, the studies on coal gasification slag mainly focused on three aspects: (1) general characterization of the slags, such as composition, morphology, physico-chemical characteristics of residual carbon, characteristics and catalytic actions of inorganic constituents, particle size distribution and thermal expansion property [15-18]. In addition, in order to improve the efficiency of coal gasification, residual carbon in the slag was investigated extensively [19, 20]; (2) rheological behavior and flow properties of the slags, which determine the slag tapping temperature in the gasifier [21-25]; (3) the utilization of the slag. Accordingly, the environmentally safe utilization of the waste slags must be addressed and developed. Recently, most of the slags were conducted in cement (39.3%), landfill (33.4%), road and flyover (5.0%), agriculture (2.9%), bricks and tiles manufacture (12.3%) [26], in addition, the SiAlON ceramics prepared by the slags were investigated by our research group [27].

Thus far, many different types of industrial wastes are used as the raw materials of foam ceramic, such as fly ash, blast furnace slag, porcelain waste etc [28-30], but there are few studies about foam ceramic based on coal gasification slags. In this work, efforts had been made to prepare foam ceramic wall material. The coal gasification slag from Xianyang chemical industry Co.

*Corresponding author:
Tel : +86 29 82205245
Fax: +86 29 82205245
E-mail: yinhongfeng@xauat.edu.cn

LTD was used as raw material and SiC was used as foaming agent. Furthermore, the high-temperature foaming process was employed. Besides, the foaming mechanism was discussed. The significance of this work lies in two aspects: First, utilization rate of the coal gasification prepared to the foam ceramic new wall material was up to 77%. As we know, coal gasification slag is an inevitable by-product from entrained-flow coal gasification, which has resulted in environmental pollution. In this paper, comprehensive utilization rate of coal gasification slag was significantly improved, which would be alleviated the environmental pollution caused by coal chemical industry; Second, the aim products in this study possess the performance such as lightweight, thermal insulation and fireproofing, which is the green product that building materials market needs today. In other words, this work not only can verify the feasibility of this foam ceramic as a new inorganic building insulation material, but also provide an important technical support for the comprehensive utilization and industrialization of foam ceramic insulation board from coal gasification slag. Moreover, it provides new ideas for the greenization of new wall materials.

Experimental Procedure

Characterization of raw materials

In this work, the primary raw material was coal gasification slag (termed as CGS), which was provided by Xianyang chemical industry co. LTD (Xianyang, Shaanxi, China). And the clay came from the local resource. Moreover, the raw materials were dried in an oven at 110 ºC for 24 h. And for the materials, X-ray fluorescence (XRF) was employed to detect the chemical composition of raw materials, and X-ray diffraction (XRD, using a D/Max 2550V, Akashima, Japan) was used to investigate the crystalline phases of them.

The results of XRF and XRD were shown in Table 1 and Fig. 1, respectively. It can be seen CGS mainly contains 38.39 wt.% SiO_2, 31.13 wt.% C and 14.66 wt.% Al_2O_3, with a small quantity of Fe_2O_3(3.39 wt.%), CaO (5.85 wt.%), K_2O (1.64 wt.%), MgO (1.02 wt.%), Na_2O (0.89 wt.%). Furthermore, high content of SiO_2 (68.56 wt.%), Al_2O_3 (17.66 wt.%) and Fe_2O_3(4.64 wt.%) contained in clay that locally produce. Besides, it is observed from Fig. 1, in CGS, the major crystalline phase is Quartz (SiO_2), while in clay, except for the Quartz (SiO_2), the $Na_{0.3}(Al,Mg)_2Si_4O_{10}(OH)_28H_2O$ and $KAl_2Si_3AlO_{10}(OH)_2$ present as well.

Preparation of samples

In this paper, the main raw material was the CGS, meanwhile, the clay was added in appropriate content, and small quantity of SiC (3 wt.%) was added as foaming agent. And the proportion of raw materials was shown in Table 2. In order to mix raw materials well together, all raw materials were milled in de-ioned water using Si_3N_4 milling media in a planetary ball mill at a constant speed of 320 rpm for 6 h. The mixed slurry was dried at 110 ºC in oven for 24 h, and sieved through a 200-mesh screen to remove agglomerations. Then, the dried materials were made into round particles by spray granulation on a disc granulator, and the particles formed by the granulator were placed in an

Table 1. The chemical composition of raw materials (wt.%)

wt.%	Fe_2O_3	TiO_2	CaO	K_2O	SiO_2	Al_2O_3	MgO	Na_2O	P_2O_5	S	C	LOI
CGS	3.39	0.72	5.85	1.64	38.39	14.66	1.02	0.89	0.25	0.13	31.13	32.57
Clay	4.64	1.60	0.35	6.15	68.56	17.66	0.68	0.02	/	/	1.34	/

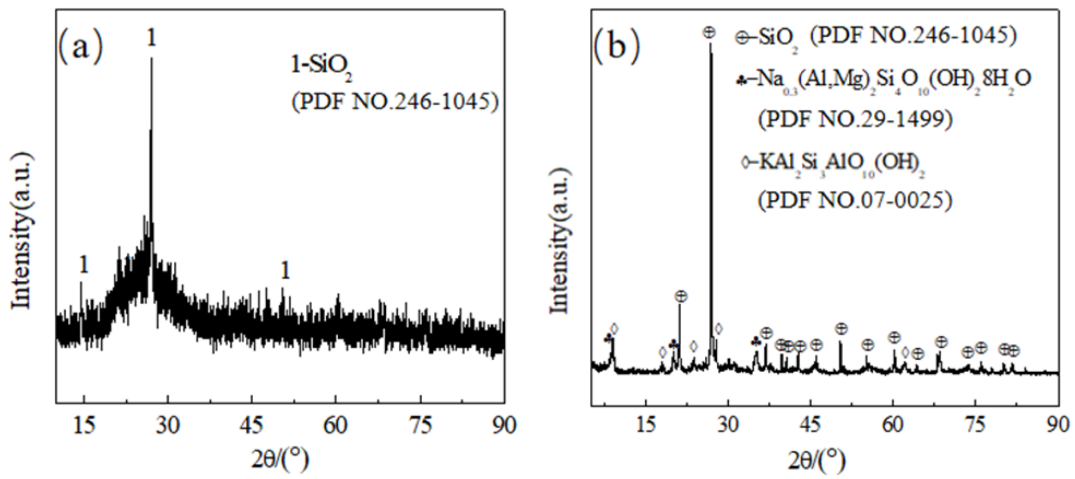

Fig. 1. X-ray diffraction of CGS (a) and clay (b).

oven to be dry at a gradient temperature (30 ºC, 50 ºC and 80 ºC for 2 h, 110 ºC for 12 h) in order to prevent the particle from cracking. After drying, three particle size distributions (1.4~2.36 mm, 1~1.4 mm and 0.25~1 mm) were obtained by passing through a sieve of 8 mesh, 12 mesh, 16 mesh and 60 mesh, respectively. Then, samples were prepared directly by heating the particles in a furnace at a various final temperature in the range of (1,140~1,160 ºC at an interval of 10 ºC). The heating rate was 5 ºC/min, and then the sintered samples were cooled naturally.

Characterization of sintered samples

For the mixed powder, in order to determine the weight losses and the thermal behavior of high temperature, the thermal gravimetric-differential scanning calorimeter analysis (TG-DSC, STA449F3, Selb, Germany) was studied. The test condition of the temperature range was from the 20 to 1,400 ºC with a heating rate of 15 ºC/min at air atmosphere.

For the sintered samples, volume density, compressive strength, thermal conductivity, phase composition and microstructure were characterized systematically. First, the volume density of the sintered samples, according to GB/T5486-2008 test method for inorganic hard adiabatic products, was evaluated [31]. In this test, the samples were dried at 110 ºC for 12h, and then restored to room temperature, then measured the weight (termed as M); The geometry of the sample were measured and its volume (termed as V) was calculated. Finally, the volume density (ρ) was calculated by using the following formula (1)

$$\rho = \frac{M}{V} \tag{1}$$

Second, compressive strength was tested by compression testing machine (Yes-600, Jinan, China), according to GB/T5486-2008 test method for inorganic hard adiabatic products as well. Third, thermal conductivity was detected by Thermal Conductivity Measuring Instrument (TC3000, Xi'an, China); Forth, Phase identification of the samples was performed via X-ray diffractometry (XRD, using a D/Max 2,550 V, Akashima, Japan) applying $CuK_{\alpha 1}$ ($\lambda = 1.5405981$ Å) radiation; And then the morphology of the samples was investigated by scanning electron microscopy (SEM, model Auriga, Zeiss, Oberkochen, Ostalbkreis, Germany).

Table 2. The weight ration of samples (wt.%)

Number	CGS	Clay	Particle size
1	77	20	0.25~1 mm
2	77	20	1.0~1.4 mm
3	77	20	1.4~2.36 mm
4	75	22	0.25~1 mm
5	82	15	0.25~1 mm

Results and Discussion

The foaming mechanism of SiC in CGS

Considering the foaming temperature of SiC is varied from 900 ºC to 1,300 ºC; Moreover, according to the previous study [30] of our research group, the lowest eutectic point of each component of CGS is 1,170 ºC. For this reason, SiC was used as the foaming agent.

For better research on the foaming mechanism of SiC in CGS, the combustion thermodynamics and kinetics for SiC were studied. The Gibbs free energy of some reactions of SiC with oxygen at 25 ºC and 1,170 ºC were calculated by FactSage 7.1 (Reaction module, Beijing, China). As displayed in Table 3, It can be obviously seen that all the Gibbs freeenergy was negative number. Therefore, based on the thermodynamics, SiC was unstable both at room temperature and the melting temperature of CGS system. And it can be reacted with oxygen and caused gas released. From a kinatics point of view, the combustion reaction of SiC was not smoothly. Numerous studies indicated that there existed a dense SiO_2 envelope layer that muffled SiC during the reaction [32, 33]. In that case, the rate of oxidation reaction between SiC and O_2 was controlled by diffusion, and what's more, the diffusion rate of oxygen in the SiO_2 envelope layer was only 10^{-14}~10^{-15} cm^2/s. Hence, SiC (inside of the raw material system) reacted with the oxygen was effectively stopped. Moreover, the TG-DSC of the raw material system from room temperature to 1,400 ºC in air atmosphere had been tested for study the reaction temperature of the raw material system and the foaming mechanism of SiC in CGS. The result was shown in Fig. 2. Intuitively, there exists a weight loss

Table 3. Reactions of SiC in 25 ºC and 1170 ºC.

Reaction	$\Delta G_T/(KJmol^{-1})$	
	25 ºC	1,170 ºC
$SiC(s)+2O_2(g)\rightarrow SiO_2(s)+CO_2(g)$	-1181.6	-977.7
$SiC(s)+3/2O_2(g)\rightarrow SiO_2(s)+CO(g)$	-924.3	-820.1

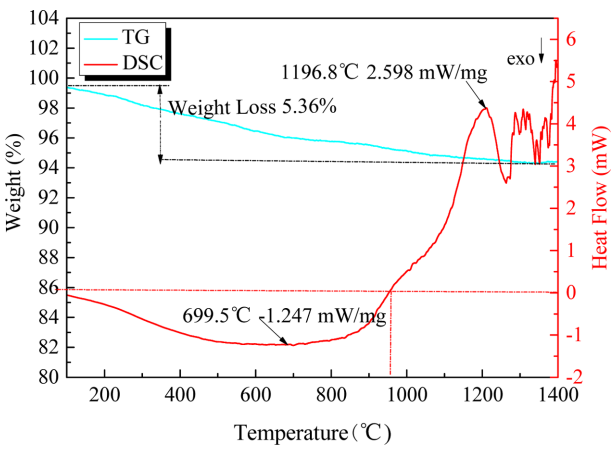

Fig. 2. The TG-DSC result of the mixed raw materials.

of 5.36% during the testing process, and this weight loss may be the impact of impurities and oxidation of residual carbon. In addition, in Fig. 2 there is an endothermic peak from 950 to 1,230 ºC, which indicates the generation of liquid phase and oxidation of SiC at this temperature range [34-36]. According to the research of Hao Wang [30], the TG-DSC of SiC from room temperature to 1,380 ºC in air atmosphere showed that the weight of the system increased; compared with the theoretical calculation, the weight increment could reach 50% when the SiC fully reacted with O_2. Nevertheless, seen from Fig. 2, there was no noticeable increase in weight for CGS system. This might be the result of the low content of SiC and higher content of residual carbon. As to the temperature of the endothermic peak, the endothermic peak of pure silicon carbide appeared at about 1,110 ºC, while the CGS system appeared at about 1,198 ºC, which could explain as follows: the simulated ternary phase diagram of the raw material system showed that the lowest eutectic point of the system was 1,170 ºC, and with the temperature increasing, the liquid phase quantity persistently increased, which would destroy the SiO_2 protective layer, in that case, the temperature was up to about 1,198 ºC, the SiC inside can reacted with oxygen sufficiently.

Hence, As displayed in Fig. 3, the preparation of foaming ceramics by the CGS system can be expressed as: Firstly, owing to contain certain SiO_2 in the system and generate the SiO_2 protective layer covered on the SiC, SiC showed relatively stable at lower temperature; Secondly, the combustion of residual carbon some extent provided the impetus for the reaction of SiC with oxygen until the residual carbon reacted completely; Thirdly, the liquid phase generated with the sintering temperature increased, which destroyed the SiO_2 protective layer and gave rise to the increase of O_2 diffusion rate, meanwhile, a capillary pressure formed by high temperature liquid phase could make sample densified and fix the gas in the liquid phase as well. In this case, the closed pores were formed in samples.

The effects of the grain size and sintering temperature on samples

In this paper, the process of spray granulation was employed. For sample 1 to 3, heating at the temperature (1,140-1,160 ºC), the effects of the grain size on samples and sintering temperature were shown in Fig. 4. Seen from Fig. 4(a), as the particle size and sintering temperature increased, the density of the samples increased. As shown in Fig. 4(b), with the increasing of the particle size, the compress strength of the samples increased, While, the compress strength of the samples decreased. This phenomenon can be explained that, the particle size is negatively correlated with the specific surface area. The smaller the particle size, the larger the specific surface area, the more fully in contact with oxygen, the higher the heat transfer efficiency, the more liquid phase can be produced at the same temperature, and the more fully reactive between SiC and O_2. In that case, the content of the pore increased. For this reason, the density of samples decreased. Meanwhile, at higher sintering temperature, temperature becomes the most important factor, so the compress strength of the samples was lowest at 1,160 ºC. Whereas, the strength still meets the standard requirements for lightweight wall materials.

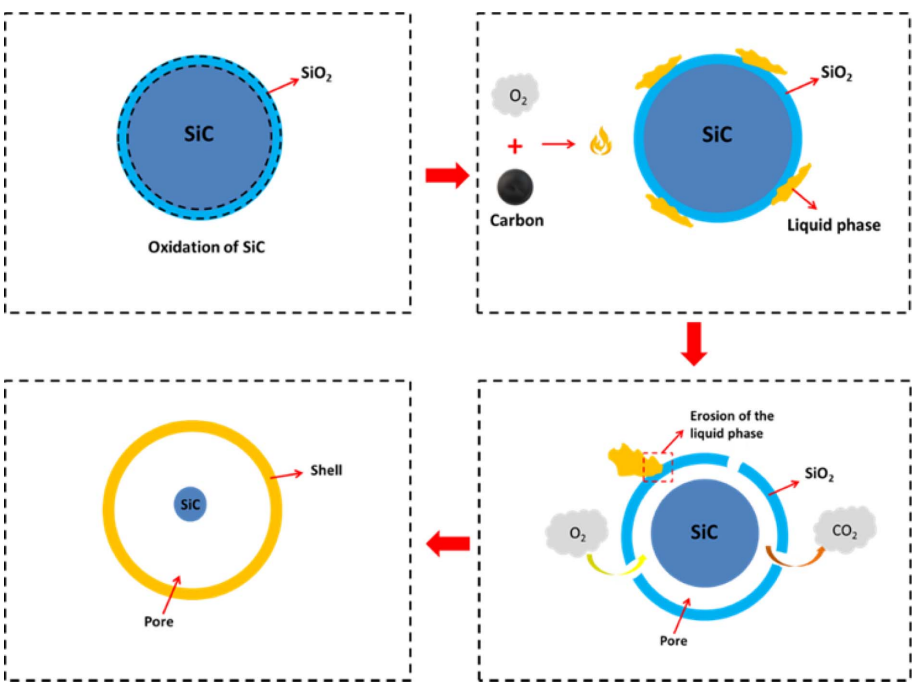

Fig. 3. Foaming mechanism of the SiC based on CGS.

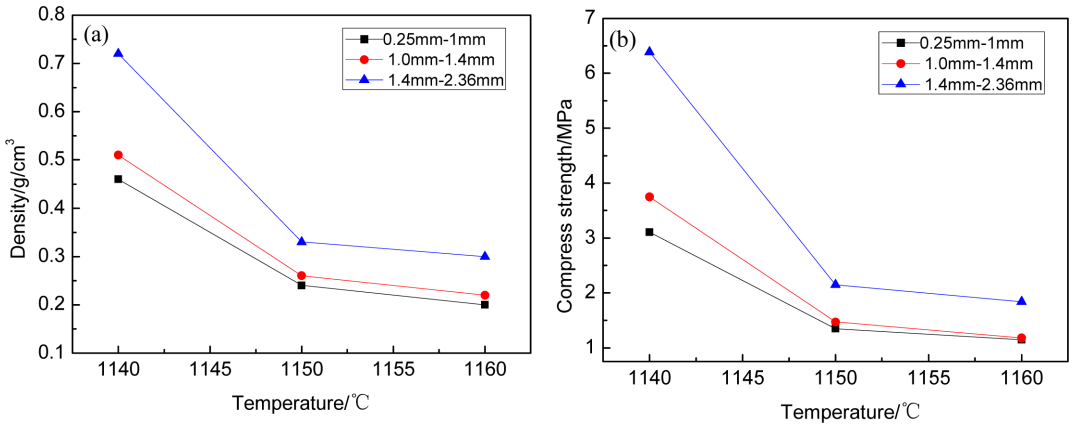

Fig. 4. The density and compress strength of samples with the varied grain size and temperature.

The effect of ratio of CGS to clay

Based on the above research, the sample prepared with the particle grain size being in the range from 0.25 to 1mm at 1,160 ºC was relatively good. Furthermore, in order to determine the utilization of CGS, the effect of the content of the CGS was investigated as well. For sample 3 to 5, with different content of CGS sintered at 1,160 ºC for 2 h, the volume density and compressive strength were detected. As displayed in Fig. 5, the value of density and compressive strength decreased with the ratio of CGS to clay raised. For CGS, there were amount of glass phase, and they could transform into liquid phase at a higher temperature, which promoted oxidation of SiC and resulted in generating more pore in samples; Meanwhile, as shown in Table 1, the clay contained more content of SiO_2 that can increase the viscosity and associativity of the reaction system. Therefore, when the ratio of CGS to clay increased, the samples become loose, and the value of density and compressive strength decreased. However, according to the literature [37], the foam ceramic can be used as walling material, it must be the value of the density less than 1 g/cm^3 and the compress strength no less than 0.6 MPa. And at the same time, given the environmental benefit, the utilization of CGS should be as high as possible. Hence, by contrast, when the ratio of CGS to clay: 77:20 was relatively reasonable.

Discuss on the optimal solution

In order to verify the feasibility of this foam ceramic as a new inorganic building insulation material. Seen from 3.1 and 3.2, the sample with ratio of CGS to clay (77:20), the particle grain size being the range from 0.25 to 1 mm, were relatively good, so the repeated experiment of the sample was carried out with the various temperature (1,140~1,160 ºC). And the performance of the products such as volume density, compressive strength, thermal conductivity, phase composition and microstructure were all characterized systematically.

Fig. 6 depicts phase composition of the sintering products at various temperature. It can be found that many crystalline minerals, such as anorthite ($CaAl_2Si_2O_8$), albite (Na (Si3Al) O_8), and SiC exist in all the products. Among them, the anorthite, as a typical ceramic phase, is formed by aluminosilicate at high temperature, which plays a key role in compress strength of the

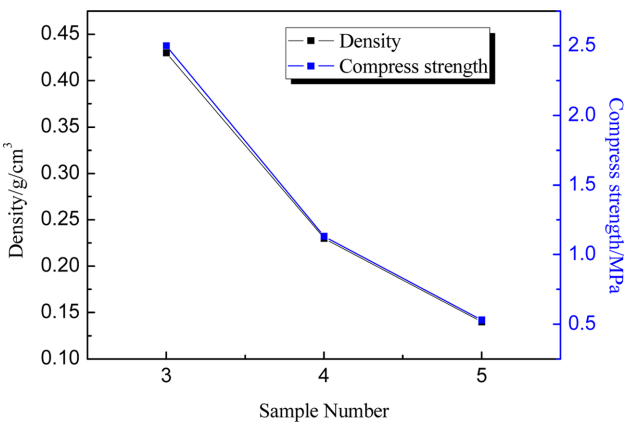

Fig. 5. The density and compress strength of samples with ratio of CGS to clay 3(72:25), 4(77:20), 5(82:15).

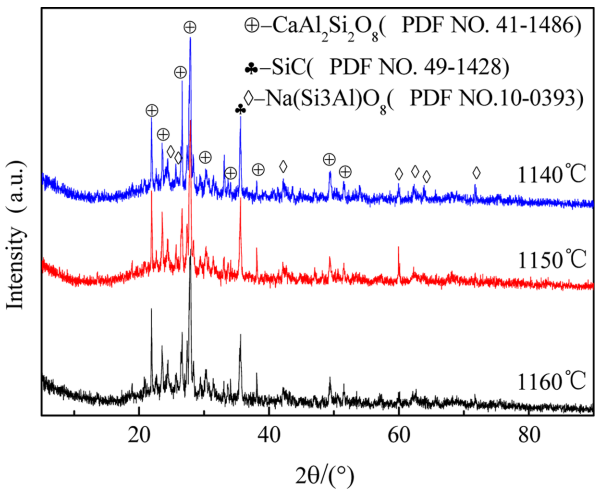

Fig. 6. X-ray diffraction of sintering products.

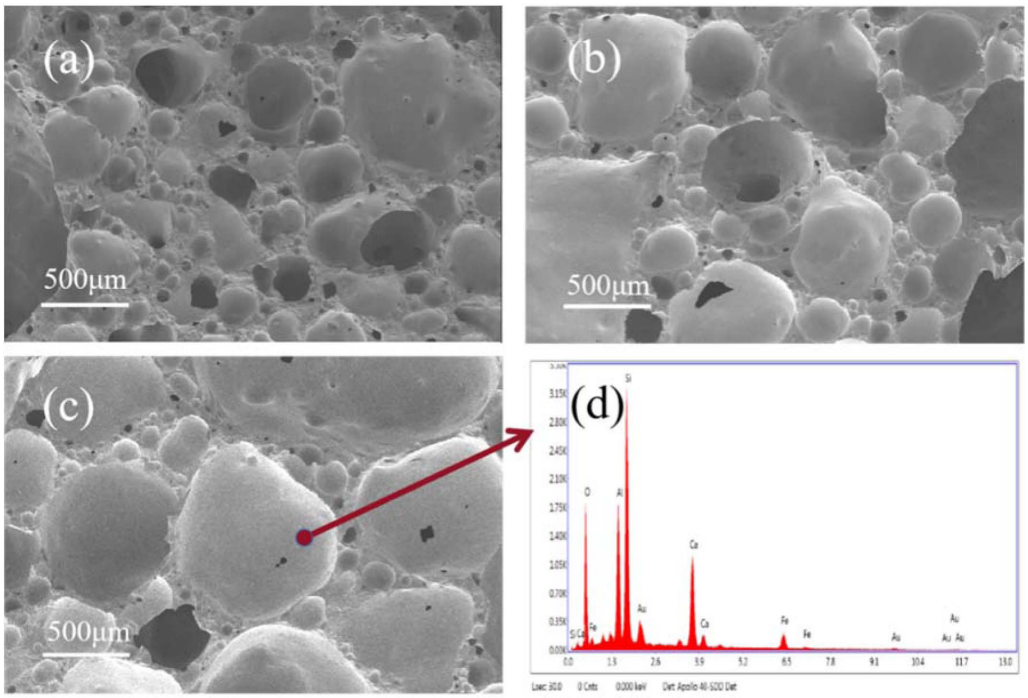

Fig. 7. SEM and EDX (d) image of samples with different sintering temperatures: (a) 1,140 ℃; (b) 1,150 ℃; (c) 1,160 ℃.

products. In addition, as displayed in Fig. 6, the content of SiC decreased with the sintering temperature increased, it indicated that, as the temperature increased, the oxidation of SiC in side became more and more complete. Hence, the result of XRD analysis is consistent with the part of 3.1.

And Fig. 7 clearly revealed the evolution of microstructure of the products sintered at various temperatures from 1,140 to 1,160 ℃. As presented in Fig. 7, almost all the pores showed roundness and closed in product at 1,160 ℃. And there were also relatively more interconnected porosity in product at 1,140 ℃ and 1,150 ℃. It can be indicated that the liquid phase got more generated and viscosity of the liquid phase decreased with sintering temperature increased [38, 39]. Thus, the liquid phase will approach particles in ceramic body owing to surface energy. Hence, the open porosity reduces [40-42]. Besides, the pore became significantly larger with the temperature increased. It demonstrated that the surface tension of the gas which generated from the oxidation of SiC caused the pores coalescing. By contrast, the content and the size of the closed pores were the most suitable for applying to thermal insulation material.

As indicated in Table 4, the density, compress strength and thermal conductivity of the products with 77% CGS sintered at various temperatures were investigated. Table 4 illustrated that the density, compress strength and thermal conductivity of the products decreased with the temperature decreased. Especially, When the product fabricated with 77% CGS sintered at 1,160 ℃, the thermal conductivity was up to 0.05 W/m·k. According to the literature [43,44], compared with organic thermal insulation material, inorganic thermal insulation material has the greatest advantage of being non-flammable burning, however, because of the disadvantage of the inorganic thermal insulation materials, such as high water absorption, high cost, heat preservation performance slightly poor, etc, the inorganic thermal insulation materials is difficult to be generalized in a large scope. As we know, for high efficiency thermal insulation material, thermal conductivity is less than 0.05 W/m·k, and for light insulation material, its thermal conductivity is less than 0.23 W/m·k [45]. Thus, the sample of this paper was fabricated by solid waste, which would not only overcome the feature of high cost for inorganic thermal insulation materials, but also process the virtue of lightweight and low thermal conductivity that close to that of high-efficiency insulation material. Hence, the samples can be expected to apply to light insulation partition panel.

Table 4. The performance of the products sintering various temperature (1,140~1,160 ℃).

Performance	1,160 ℃	1,150 ℃	1,140 ℃
Density (g/cm^3)	0.21	0.35	0.50
Compress strength (MPa)	1.18	1.41	3.35
Thermal conductivity (W/m·k)	0.05	0.08	0.13

Conclusions

In conclusion, this research emphasized the viability of recycling CGS from chemical plant to produce foam

ceramic new wall material using SiC as foaming agent. It can be indicated that: the optimum particle size rang was 0.25~1 mm, at the sintering temperature was 1,160 ºC, the foam ceramic new wall material with 77% CGS presented relatively low volume density of 0.21 g/cm^3, low heat conductivity coefficient of 0.05 W/(m·k), and the corresponding compress strength of 1.18 MPa. Moreover, the total amount of CGS is up to 77%, which greatly reduces the cost of raw materials and has played a very beneficial role in environmental protection. Finally, it will have great potential in the application in the field of new building materials.

Funding

This work was financially supported by the Joint Funds of the National Natural Science Foundation of China (No. U1261118).

References

1. T.E. Peng, H.C. Li, Y.L. Liu, Y.L.Wang, and L. Liu, Ceramics 12 (2019) 00-00.
2. X.J. Mao, S.W. Wang, and J.Z. Daojing, in Proceedings of the 2006 Beijing International Materials Week, June 2006, edited by S. Long, X. Zhang, Y. Han, C. Peng, Y. Lu (Trans Tech Publications Limited, 2007) p.00.
3. L. Chen, Y. Li, and W. Liu, J. Ceram. 4 (2011) 116-120.
4. X. Liu, H. Li, X. Gao, X. Li, L. Wang, H. Duan, and X.G. Li, Chemical Industry Progress 11 (2012) 167-172.
5. Y.F Dong, X.Y. Wang, Z.H. Li, S. Liu, and C.C. Liu, Ceramics 7 (2007) 54-56.
6. F.F Jiao and G.Y. Zhu. Ceramics 8 (2007) 9-11.
7. A. Pokhrel, J.G. Park, S.M. Park, and I.J. Kim, J. Ceram. Process. Res. 14[4] (2013) 502-507.
8. J.G. Park, A. Pokhrel, S.D. Nam, and W. Zhao, J. Ceram. Process. Res. 14[4] (2013) 508-512.
9. L. Li, in "Preparation and properties of CWS/silicate foaming materials" (Qingdao University Press, 2017) p.00.
10. A.M. Bernardin, M.J.D. Silva, and H.G. Riella, J. Mater. Sci. Eng. A 437[2] (2006) 222-225.
11. H.R. Femandes, D.U. Tulyaganov, and J.M.F. Ferreira, Ceram. Int. 35[1] (2009) 229-235.
12. J. Luyten, S. Mullens, J. Cooymans, A.M. De Wilde, I. Thijs, and R. Kemps, J. Eur. Ceram. Soc. 29[5] (2009) 829-832.
13. Z.N. Ye, Y.W. Wang, H. Jiang, N. Li, and S.Q. Liu, Key Eng. Mater. 575-576 (2013) 461-464.
14. A. Acosta, M. Aineto, I. Iglesias, M. Romero, and J.M. Rincón, Mater. Lett. 50 (2001) 246-250.
15. V. Choudhry, S. Kwan, and S.R. Hadley, in "Utilization of lightweight materials made from coal gasification slags; Technical Report" (Praxis engineers, 2001) p.00.
16. A. Acosta, I. Iglesias, M Aineto, M. Romero, and J.M. Rincón, J. Therm. Anal. Calorim. 67 (2002) 249-255.
17. M. Aineto, A. Acosta, J.M. Rincón, and M. Romero, Fuel 85 (2006) 2352-2358.
18. N.J. Wagner, R.H. Matjie, J.H. Slaghuis, and J.H.P. van Heerden, Fuel 87 (2008) 683-691.
19. T. Wu, M. Gong, E. Lester, F.C. Wang, Z.J. Zhou, and Z.H. Yu, Fuel 86 (2007) 972-982.
20. S.Q. Xu, Z.J. Zhou, X.X. Gao, G.S. Yu, and X. Gong, Fuel Process. Technol. 90 (2009) 1062-1070.
21. W.J. Song, L.H. Tang, X.D. Zhu, Y.Q. Wu, Z.B. Zhu, and S. Koyama, Fuel 89 (2010) 1709-1715.
22. W.J. Song, L.H. Tang, X.D. Zhu, Y. Wu, Y. Rong, Z. Zhu, andS. Koyama. Fuel 88 (2009) 297-304.
23. G.S. Yu, Q.R. Zhu, G.Z. Chi, Q.H. Guo, and Z.J. Zhou, Fuel Process. Technol. 104 (2012) 136-143.
24. L.X. Kong, J. Bai, Z.Q. Bai, Z. Guo, and W. Li, Fuel 108 (2013) 76-85.
25. Y. Tang, H.F. Yin, H.D. Yuan, H. Shuai, and Y.L. Xin, Adv. Powder Technol. 27 (2016) 2232-2237.
26. M.J. Du, J.J. Huang, Z.Y. Liu, X. Zhou, S. Guo, Z.Q. Wang, and Y.T. Fang, Fuel 224 (2018) 178-185.
27. H.F. Yin, Y. Tang, J.Z. Zhang, and J. Chin, Ceram. Soc. 39 (2011) 233-238.
28. L. Ding, W. Ning, Q.W. Wang, D.N. Shi, and L.D. Luo, Mater. Lett. 141[15] (2015) 327-329.
29. X. Chen, A. Lu, and G. Qu, Ceramics International 39[2] 92013) 1923-1929.
30. H. Wang, Z. Chen, L.L. Liu, R. Ji, and X.D. Wang, Ceram. Int. 44 (2018) 10078-10086.
31. Chinese Standard, No. GB/T5486-2008 (2008) p.00.
32. X. Xi, L. Xu, A.Z. Shui, Y.M. Wang, and M. Naito, Ceram. Int. 40 (2014) 12931-12938.
33. X. Xi, A. Shui, Y.F. Li, Y.M. Wang, H. Abe, and M. Naito, J. Eur. Ceram. Soc. 32 (2012) 3035-3041.
34. T.W. Cheng and Y.S. Chen, Ceram. Int. 30 (2004) 343-349.
35. B. Chen, K. Wang, X.J. Chen, and A.X. Lu, Mater. Lett. 79 (2012) 263-265.
36. H. Wang, M. Zhu, Y.Q. Sun, R. Ji, L.L. Liu, and X.D. Wang, Constr. Build. Mater. 155 (2017) 930-938.
37. Y.P. Feng, H.F. Yin, H.D. Yuan, L. Zhang, and H. Cui, Silicate Bulletin 3 (2014) 55-59.
38. H. Shuai, H.F. Yin, and H.D. Yuan, Coal Convers. 38 (2015) 44-48.
39. H.D. Yuan, H.F. Yin, Y. Tang, H. Shuai, and Y.L. Xin, Materials 13[6] (2020) 1346.
40. S. Kumar, K.K. Singh, and P. Ramachandrarao, J. Mater. Sci. 36[24] (2001) 5917-5922.
41. F.J. Torres, E.R.D. Sola, and J. Alarcón, J. Eur. Ceram. Soc. 26[12] (2006) 2285-2292.
42. T.K. Mukhopadhyay, S. Ghosh, J. Ghosh, S. Ghatak, and H.S. Maiti, Ceram. Int. 36[3] (2010) 1055-1062.
43. Q.W. Zhu, F.D. Wu, and J.P. Zhao, New Build. Mater. 6 (2012) 12-16.
44. M.S. Al-Homoud, Build. Environ. 40[3] (2005) 353-366.
45. B.P. Jelle, Energy Build. 43[10] (2011) 2549-2563.